Transformation of the cerebellum into more ventral brainstem fates causes cerebellar agenesis in the absence of *Ptf1a* function

Kathleen J. Millen[a,b,1], Ekaterina Y. Steshina[c], Igor Y. Iskusnykh[c], and Victor V. Chizhikov[c,1]

[a]Seattle Children's Research Institute, Seattle, WA 98101; [b]Department of Pediatrics, University of Washington, Seattle, WA 98101; and [c]Department of Anatomy and Neurobiology, University of Tennessee Health Science Center, Memphis, TN 38163

Edited by Kathryn V. Anderson, Sloan–Kettering Institute, New York, NY, and approved March 19, 2014 (received for review August 28, 2013)

Model organism studies have demonstrated that cell fate specification decisions play an important role in normal brain development. Their role in human neurodevelopmental disorders, however, is poorly understood, with very few examples described. The cerebellum is an excellent system to study mechanisms of cell fate specification. Although signals from the isthmic organizer are known to specify cerebellar territory along the anterior–posterior axis of the neural tube, the mechanisms establishing the cerebellar anlage along the dorsal–ventral axis are unknown. Here we show that the gene encoding pancreatic transcription factor PTF1A, which is inactivated in human patients with cerebellar agenesis, is required to segregate the cerebellum from more ventral extracerebellar fates. Using genetic fate mapping in mice, we show that in the absence of *Ptf1a*, cells originating in the cerebellar ventricular zone initiate a more ventral brainstem expression program, including LIM homeobox transcription factor 1 beta and T-cell leukemia homeobox 3. Misspecified cells exit the cerebellar anlage and contribute to the adjacent brainstem or die, leading to cerebellar agenesis in *Ptf1a* mutants. Our data identify *Ptf1a* as the first gene involved in the segregation of the cerebellum from the more ventral brainstem. Further, we propose that cerebellar agenesis represents a new, dorsal-to-ventral, cell fate misspecification phenotype in humans.

human cerebellar malformation | mouse | neuronal progenitors | neuronal specification | dorsal–ventral patterning

Proper cell fate specification decisions are critical for the development of the vertebrate central nervous system (CNS). Misregulation of cell fate results in the generation of abnormal neuronal populations and, in extreme cases, can transform one brain region into another one (1–5). Analyses in model organisms have revealed the molecular mechanisms of some cell fate specification decisions in the developing CNS, including, for example, hindbrain patterning by homeobox (*Hox*) genes (3–5). Disruptions of cell fate specification have long been hypothesized to contribute to human developmental brain disorders (6, 7). To date, however, very few examples of neuronal misspecification have been documented in patients, and the role of aberrant cell fate decisions in human brain developmental pathogenesis remains largely unknown.

The developing cerebellum is an excellent system to study cell fate regulation. It is composed of very few neuronal cell types, and its developmental neuroanatomy is well defined (8). During development, cerebellar neurons originate from one of two germinal zones in the cerebellar anlage in the alar plate of rhombomere 1 (rh1): the cerebellar ventricular zone (VZ) and the cerebellar rhombic lip (RL). The cerebellar RL arises adjacent to the fourth ventricle roof plate. It produces glutamatergic neurons, such as glutamatergic neurons of the deep cerebellar nuclei (DCN), granule cells, and unipolar brush cells (UBCs) (9–14). RL-derived cells also contribute to the fourth ventricle roof plate and its later derivative the choroid plexus (15). The cerebellar VZ gives rise to GABAergic cerebellar neurons, such as Purkinje cells, GABAergic neurons of DCN, and molecular layer interneurons (16–18).

In the developing CNS, the position and extent of the cerebellar anlage are precisely regulated. The isthmic organizer and a cascade of related genes have been identified as key regulators establishing the cerebellar territory along the anterior–posterior (A–P) axis of the CNS (1, 2, 8, 19). In contrast, the mechanisms that establish the cerebellar anlage along the dorsal–ventral (D–V) axis of the neural tube are unknown. Furthermore, it is currently unclear which cells originate from the domain located directly ventral to the cerebellar anlage, thus complicating the identification of the mechanisms segregating the cerebellum from more ventral extracerebellar cell fates.

Developmental cerebellar malformations are relatively common in humans. Genes for several of these clinically important malformations have been identified over the last decade (6, 7). One such gene is *PTF1A*, encoding a basic helix–loop–helix (bHLH) transcription factor. Inactivation of *PTF1A* causes cerebellar agenesis (20–22). Analysis in mice has shown that *Ptf1a* is specifically expressed in the cerebellar VZ. In the absence of *Ptf1a*, some VZ-derived cells die (16, 23), whereas others adopt the fate of granule neuron precursors, which normally originate from the more dorsally located RL (23).

Although the intracerebellar VZ to RL transformation phenotype in *Ptf1a* mutants is striking, here we show that relatively few mutant cells actually undergo this transformation. Using our newly developed gene expression map of intermediate rh1 and genetic fate mapping in mice (24), we instead demonstrate that *Ptf1a* mutant cerebellar agenesis is caused by an early and funda-

Significance

The contribution of cell fate misspecification to human brain disorders is poorly understood. The cerebellum, a major center of motor and sensory coordination, is frequently malformed in humans. During development it arises from dorsal hindbrain, but a long-standing question has been how the cerebellum is established along the dorsal–ventral axis of the neural tube. Here we identified the gene encoding pancreatic transcription factor PTF1A, which is inactivated in patients with cerebellar agenesis, as the first gene regulating the ventral limit of the cerebellum. We describe transformation of cerebellar neurons into more ventral extracerebellar fates as a novel mechanism of cerebellar agenesis. Our data provide some of the strongest evidence reported to date for a critical role of cell fate misspecification in a human brain developmental phenotype.

Author contributions: K.J.M. and V.V.C. designed research; K.J.M., E.Y.S., I.Y.I., and V.V.C. performed research; K.J.M., E.Y.S., and V.V.C. analyzed data; and K.J.M. and V.V.C. wrote the paper.

The authors declare no conflict of interest.

This article is a PNAS Direct Submission.

[1]To whom correspondence may be addressed. E-mail: kathleen.millen@seattlechildrens.org or vchizhik@uthsc.edu.

This article contains supporting information online at www.pnas.org/lookup/suppl/doi:10.1073/pnas.1315024111/-/DCSupplemental.

mental fate switch from cerebellar to more ventral extracerebellar cell fates. Our data highlight the remarkable developmental plasticity of the cerebellar VZ and introduce cell fate transformation from the cerebellum to brainstem as a novel mechanism of cerebellar pathology in humans.

Results

Only a Small Fraction of Cerebellar VZ Progenitors Adopt Cerebellar Granule Cell Fates in *Ptf1a*$^{-/-}$ Mutants. Previous analysis of *Ptf1a* mutant mice revealed that in the absence of *Ptf1a* function, the cerebellar VZ abnormally produces granule cell precursors instead of GABAergic cerebellar neurons (23). We confirmed this finding (Fig. 1 *A–D*) using *Ptf1a*$^{Cre/Cre}$ (*Ptf1a*$^{-/-}$)/*ROSA* embryos, in which *Ptf1a*-expressing progenitors in the cerebellar VZ and their progeny were permanently labeled with cytoplasmic β-gal expression from the *ROSA26* allele (25). Surprisingly, however, we noted that only a small fraction (~12%) of the β-gal+ cells in embryonic day 15 (e15.0) *Ptf1a*$^{Cre/Cre}$;*ROSA* (*Ptf1a*$^{-/-}$) rh1 were located in the external granule cell layer (EGL), the location of all granule cell progenitors at this developmental stage (Fig. 1 *D*,

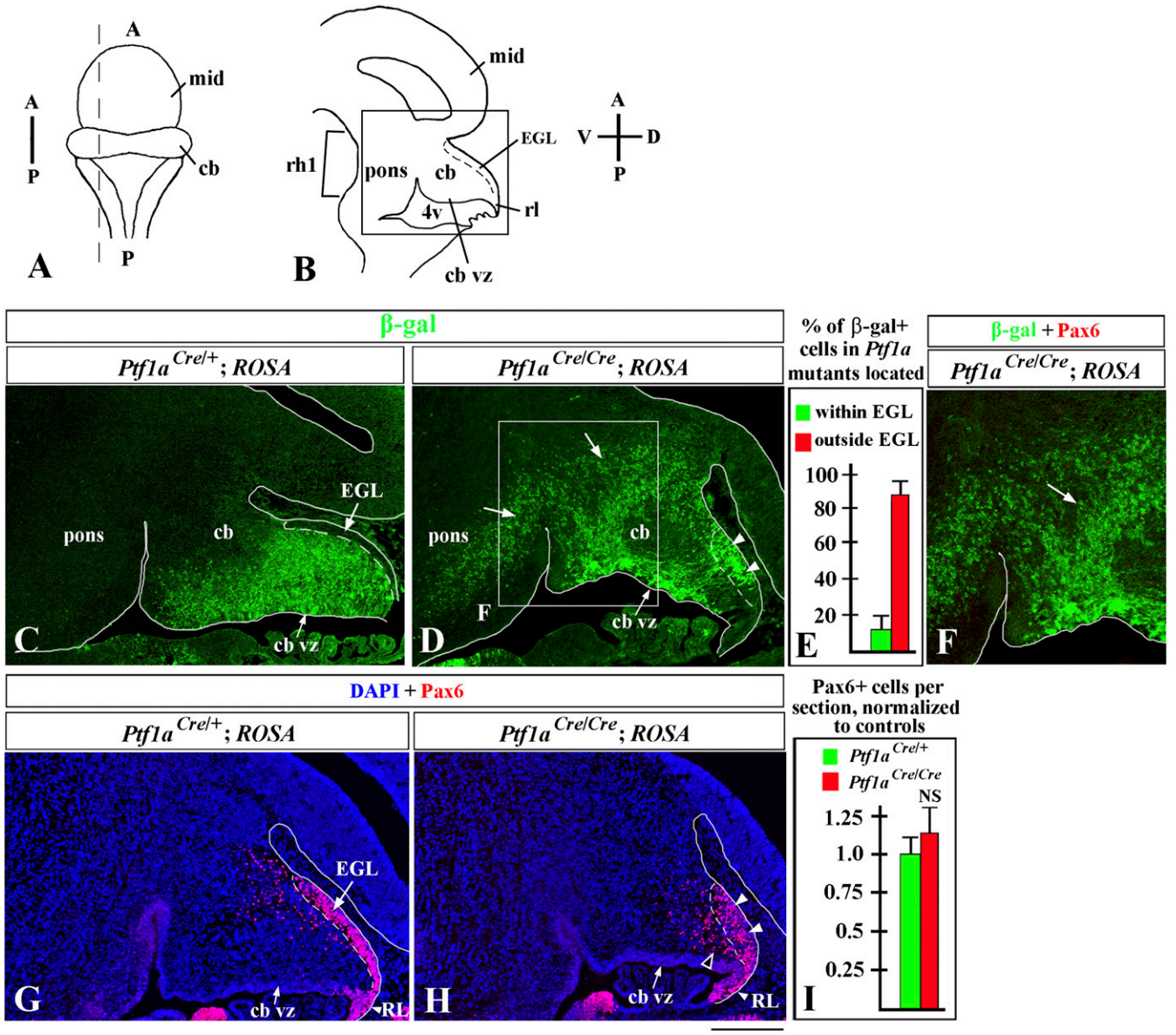

Fig. 1. In the absence of Ptf1a, cerebellar VZ derivatives become more broadly distributed in rh1, but only a minority adopt granule cell progenitor fates. (*A*) Schematic of a dorsal whole mount view and (*B*) sagittal section of the mid/hindbrain region at the level of the dashed line in *A*. Axes, midbrain (mid), cerebellum (cb), pons, rh1, fourth ventricle (4v), cerebellar VZ (cb vz), RL, and EGL are labeled. (*C*, *D*, *G*, and *H*) Sagittal sections of e15.0 embryos, corresponding to the region boxed in *B*, with genotypes and antibody markers indicated. (*C*) In *Ptf1a*$^{Cre/+}$;*ROSA* (control) embryos, the EGL (demarcated by dashed line) was β-gal−, and β-gal+ cells were located within the cerebellum (cb). (*D*) In *Ptf1a*$^{Cre/Cre}$;*ROSA* (*Ptf1a*$^{-/-}$) embryos, the EGL contained β-gal+ cells (arrowheads), but many β-gal+ cells were located in ectopic anterior and ventral positions (arrows), some clearly outside the cerebellum (left arrow). (*E*) Quantification of β-gal+ cells located within the EGL and outside the EGL in *Ptf1a*$^{Cre/Cre}$;*ROSA* (*Ptf1a*$^{-/-}$) embryos ($n = 4$ embryos). (*F*) Boxed region from *D*. Many β-gal+ cells in *Ptf1a*$^{Cre/Cre}$;*ROSA* (*Ptf1a*$^{-/-}$) rh1 located outside the EGL were negative for the granule cell marker Pax6 (arrow). (*G* and *H*) In *Ptf1a*$^{-/-}$ (*Ptf1a*$^{Cre/Cre}$) cerebella, the EGL was thicker but shorter (*H*, arrowheads) than in controls. Open arrowhead (*H*) points to ectopic Pax6+ cells adjacent to a dorsal segment of the cerebellar VZ. (*I*) Quantification of Pax6+ cells per sagittal cerebellar section revealed no statistically significant differences (NS, nonsignificant; $P = 0.18$; $n = 6$ embryos for each genotype) between e15.0 *Ptf1a*$^{Cre/+}$ and *Ptf1a*$^{Cre/Cre}$ (*Ptf1a*$^{-/-}$) embryos. [Scale bar, 200 μm (*C*, *D*, *G*, and *H*) and 130 μm (*F*).]

arrowheads, and *E*). The vast majority (~88%) of β-gal+ cells in $Ptf1a^{-/-}$ rh1 were located outside the EGL (Fig. 1 *D* and *E*) and failed to express the granule cell progenitor marker Pax6 (Fig. 1*F*, arrow), suggesting that they had not adopted granule cell fate.

To further assess granule cell development in the absence of Ptf1a function, we analyzed the RL and EGL in *Ptf1a* mutants. Immunohistochemistry with antibodies against transcription factors Pax6, LIM homeobox transcription factor 1 alpha (Lmx1a), and Tbr2, which label progenitor populations in the RL (11, 12, 26), did not reveal gross RL disruptions in e14.5 $Ptf1a^{-/-}$ embryos (Fig. S1). In e15.0 *Ptf1a* mutants, however, the Pax6+ EGL was thick and short (Fig. 1 *G* and *H*), and ectopic Pax6+ cells were found adjacent to a dorsal segment of the cerebellar VZ (Fig. 1*H*, open arrowhead). Importantly, cell counts revealed only a modest and nonsignificant ($P = 0.18$) increase in the number of Pax6+ cells in $Ptf1a^{-/-}$ ($Ptf1a^{Cre/Cre}$) cerebella relative to control ($Ptf1a^{Cre/+}$) cerebella (Fig. 1 *G*–*I*). It is likely that the eventual granule cell phenotype in *Ptf1a* mutants is caused by complex mechanisms. For example, the total number of granule cells in the $Ptf1a^{-/-}$ cerebellum and EGL morphology is likely affected by ectopic granule cells arising from the cerebellar VZ. At the same time, we cannot exclude the possibility that abnormalities in the $Ptf1a^{-/-}$ cerebellar VZ also nonautonomously affect granule cell development. Nevertheless, the fact that we did not observe a significant increase in the number of Pax6+ cells in *Ptf1a* mutants supports our fate mapping result that in the absence of *Ptf1a*, only a minor fraction of cerebellar VZ cells become granule cells.

Interestingly, many β-gal+ cells located outside the EGL in $Ptf1a^{Cre/Cre}$;*ROSA* ($Ptf1a^{-/-}$) embryos occupied more anterior and ventral positions relative to those in corresponding sections from control $Ptf1a^{Cre/+}$;*ROSA* embryos (Fig. 1 *C* and *D*, arrows). Some of these cells were located adjacent to but clearly outside the cerebellar anlage (Fig. 1*D*, left arrow), suggesting abnormal migration of these cells in *Ptf1a* mutants. This fate mapping experiment, however, was conducted by comparing *Ptf1a* mutants with two copies of *Cre* ($Ptf1a^{Cre/Cre}$ embryos) to control embryos with one *Cre* copy ($Ptf1a^{Cre/+}$ embryos). To ensure that increased *Cre* dosage did not contribute to the broader β-gal staining observed in $Ptf1a^{Cre/Cre}$ embryos, we also studied $Ptf1a^{Cre/YFP}$ ($Ptf1a^{-/-}$) mutants with one copy of *Cre*. Indeed, by analyzing sagittal sections taken at comparable medial–lateral (M–L) levels, we found similar distribution of β-gal+ cells in $Ptf1a^{Cre/YFP}$ and $Ptf1a^{Cre/Cre}$ mice. For example, in e14.5 $Ptf1a^{Cre/YFP}$;*ROSA* ($Ptf1a^{-/-}$) embryos, many β-gal+ cells were still found outside the cerebellar anlage, in more anterior and ventral positions compared with control embryos (Fig. S2 *A* and *B*). Thus, the broader distribution of β-gal+ cells in $Ptf1a^{Cre/Cre}$;*ROSA* mutant embryos likely results from loss of Ptf1a function rather than an increased Cre dosage in these mutants.

The ventral and anterior location shift of β-gal+ cells in $Ptf1a^{Cre/YFP}$;*ROSA* ($Ptf1a^{-/-}$) mutants was widespread, throughout almost the entire M–L axis of rh1, except its most medial part (Fig. S2 *A*–*D*). In most medial $Ptf1a^{-/-}$ rh1, the β-gal+ cell population was slightly expanded anteriorly but not ventrally (Fig. S2 *C* and *D*, arrow), likely because the cerebellar anlage is separated from the pons by the aqueduct at this level.

To confirm that the broader distribution of β-gal+ cells in $Ptf1a^{-/-}$ embryos was indeed caused by abnormal migration of cells derived from the cerebellar VZ rather than by a broader labeling of progenitors in $Ptf1a^{-/-}$ mutants at an earlier stage, we analyzed embryos at e12.0, before extensive migration. At e12.0, we did not observe dramatic differences in the distribution of the initially marked population between $Ptf1a^{Cre/YFP}$;*ROSA* ($Ptf1a^{-/-}$) and control $Ptf1a^{Cre/+}$ littermates (Fig. S3), further supporting our conclusion that in older $Ptf1a^{-/-}$ embryos β-gal+ cells are found in ectopic positions because they migrate abnormally from the mutant cerebellar VZ.

In conclusion, our data suggest that in the absence of *Ptf1a* many cells derived from the cerebellar VZ occupy ectopic positions, with some cells exiting the cerebellar anlage. Although the ectopic position of these cells is consistent with the hypothesis of a cell fate switch, the majority of the *Ptf1a*-lineage cells do not adopt granule cell fates in the absence of *Ptf1a*.

A Small Fraction of Cerebellar VZ Progenitors Aberrantly Adopt Glutamatergic DCN and UBC Cell Fates in the Absence of *Ptf1a*. Granule neuron precursors share a RL developmental origin with glutamatergic neurons of the DCN and UBCs (9–14). Therefore, we tested if the $Ptf1a^{-/-}$ cerebellar VZ produces these other RL fates using a *Tau–nLacZ* Cre reporter, in which a ubiquitous neuronal *Tau* promoter drives expression of a *LoxP–Stop–LoxP–nLacZ* cassette (27). This reporter permanently labels differentiated neuronal progeny of Cre-expressing cells with nuclear β-gal expression, allowing precise identification of β-gal+ cells when colabeled for other nuclear markers (27). To ensure that the *Tau–nLacZ* reporter was suitable, we crossed *Tau–nLacZ* mice with $En1^{Cre}$ mice, which express Cre in most rh1 cells (28). We confirmed that $En1^{Cre}$;*Tau–nLacZ* e15.0–e18.5 embryos demonstrated efficient labeling of multiple neuronal rh1 populations, including glutamatergic DCN neurons, UBCs, and other neurons assessed in this study.

To determine if the $Ptf1a^{-/-}$ cerebellar VZ ectopically produced glutamatergic neurons of DCN and UBCs, we analyzed $Ptf1a^{Cre/Cre}$;*Tau–nLacZ* embryos at e15.0. In these embryos, ~5% of the β-gal+ cells expressed transcription factor Tbr1 (Fig. 2 *A*–*E*), a marker of glutamatergic DCN neurons (12). An even smaller fraction of β-gal+ cells (less than 1%) expressed Tbr2 (Fig. 2 *G*–*I*), a marker of UBCs (11). In littermates with Ptf1a function ($Ptf1a^{Cre/+}$;*Tau–nLacZ*), we did not detect β-gal+ cells colabeled with either Tbr1 or Tbr2 (Fig. 2 *A*, *B*, and *G*). Cell counts did not reveal a significant increase in the number of Tbr1+ DCN cells or Tbr2+ UBCs in $Ptf1a^{-/-}$ ($Ptf1a^{Cre/Cre}$;*Tau–nLacZ*) embryos compared with control ($Ptf1a^{Cre/+}$;*Tau–nLacZ*) littermates (Fig. 2 *F* and *J*). Thus, our fate mapping results indicate that in the absence of Ptf1a function, the cerebellar VZ produces not only granule cells but also other RL derivatives including glutamatergic DCN neurons and UBCs. Cell counts, however, suggest that the number of Tbr1+ and Tbr2+ cells that ectopically arise in the $Ptf1a^{-/-}$ cerebellar VZ is very small.

In Wild-Type Mice, a Domain, Located Directly Ventral to the Ptf1a+ Cerebellar VZ, Gives Rise to Extracerebellar Neurons. The observation that many cerebellar VZ-derived cells were shifted ventrally in *Ptf1a* mutants (Fig. 1 *C* and *D*) suggested that they were misspecified into neurons normally originating from a more ventral rh1 domain. However, the precise developmental origin of most noncerebellar neuronal populations in rh1 is poorly understood. To molecularly define the neuroepithelial populations located immediately ventral to the Ptf1+ cerebellar VZ in rh1 alar plate, we analyzed the expression of several transcription factors in wild-type mouse embryos at e12.5. We noted that progenitors in the cerebellar VZ coexpressed Ptf1a and achaete-scute complex homolog 1 (Ascl1). However, a limited domain of high Ascl1 expression, which did not express Ptf1a ($Ascl1^{high}$/Ptf1a−), was detected in the rh1 neuroepithelium immediately ventral to the Ptf1a+ cerebellar VZ (Fig. 3 *A*, green arrowhead, and *B*). Labeling with Lmx1b and paired-like homeobox 2a (Phox2a) antibodies revealed two populations of neurons apparently streaming away from the $Ascl1^{high}$/Ptf1a− progenitor domain (Fig. 3 *A*–*D*). One population expressed Phox2a, and also barely detectable levels of Lmx1b (referred to as Phox2a+ neurons below) (Fig. 3 *C* and *D*, red arrowhead). The second population expressed high levels of Lmx1b and was Phox2a− (referred to as Lmx1b+) (Fig. 3 *C* and *D*, green arrowhead). Many Lmx1b+ cells coexpressed another transcription

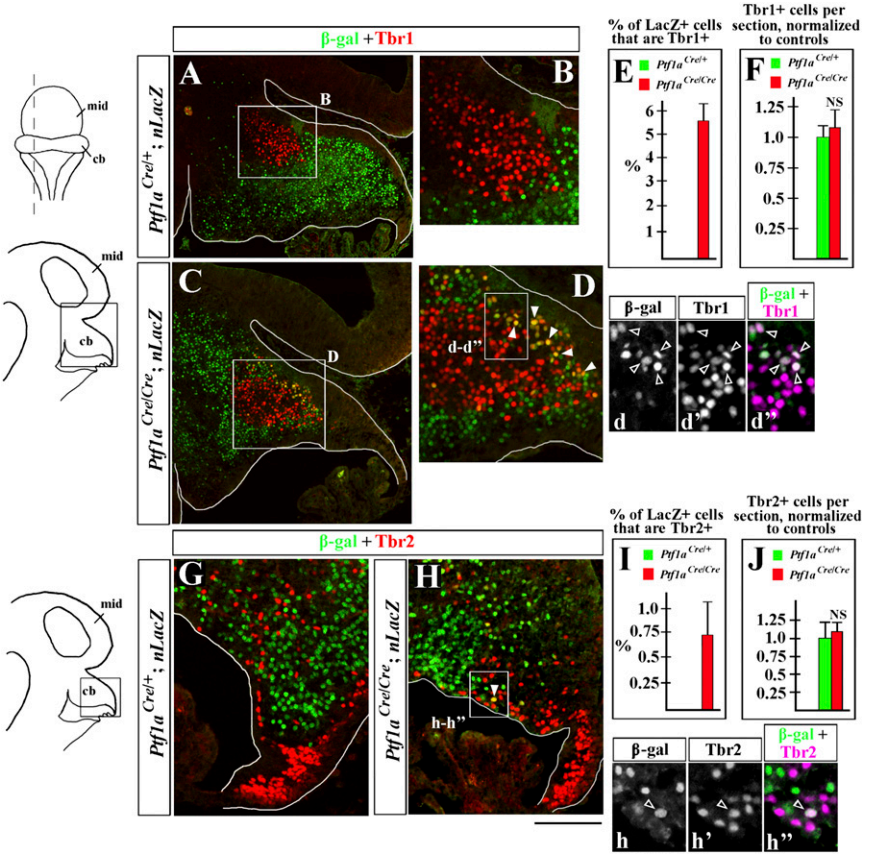

Fig. 2. Cerebellar VZ progenitors produce glutamatergic neurons of DCN and UBCs in the absence of Ptf1a function. (*A*, *C*, *G*, and *H*) Sagittal sections of e15.0 cerebellar anlage regions illustrated in schematics stained with indicated antibodies. Higher magnification images (*B*, *D*, *d–d''*, and *h–h''*) show regions boxed in adjacent panels. (*A–D*, *d–d''*, *G*, *H*, and *h–h''*) In *Ptf1a*$^{Cre/Cre}$;*Tau–nLacZ* (*Ptf1a*$^{-/-}$) but not control embryos, some β-gal+ cells expressed Tbr1 (*D* and *d–d''*, arrowheads) and Tbr2 (*H* and *h–h''*, arrowheads). β-gal+/Tbr1+ and β-gal+/Tbr2+ double-positive cells are yellow in *D* and *H* and whitish in *d''* and *h''*. (*E* and *I*) Cell counts revealed that only ~5% of β-gal+ cells expressed Tbr1 (*E*) and <1% of β-gal+ cells expressed Tbr2 (*I*) in *Ptf1a*$^{-/-}$ embryos ($n = 4$ embryos). (*F* and *J*) Quantification of Tbr1+ cells (*F*) and Tbr2+ cells (*J*) per sagittal section revealed no statistically significant difference (NS, nonsignificant; $P = 0.27$ for Tbr1+ cells, $n = 6$ embryos of each genotype, and $P = 0.7$ for Tbr2+ cells, $n = 4$ embryos of each genotype) between *Ptf1a*$^{Cre/+}$;*Tau–nLacZ* and *Ptf1a*$^{Cre/Cre}$;*Tau–nLacZ* (*Ptf1a*$^{-/-}$) embryos. [Scale bar, 200 μm (*A* and *C*), 95 μm (*B*, *D*, *G*, and *H*), 60 μm (*d–d''*), and 50 μm (*h–h''*).]

factor, T-cell leukemia homeobox 3 (Tlx3), although some cells expressed only one marker (either Lmx1b or Tlx3) (Fig. 3*E*).

To confirm that the Lmx1b+ and Phox2a+ neurons in e12.5 rh1 originated from the Ascl1^{high}/Ptf1a− VZ domain, we performed genetic fate mapping using either *Ptf1a*$^{Cre/+}$/*ROSA* or *Ascl1-Cre*/*ROSA* mouse embryos (29). Both Lmx1b+ and Phox2a+ populations were β-gal+ in *Ascl1-Cre*/*ROSA* embryos (Fig. 3 *F* and *H*), but were β-gal− in *Ptf1a*$^{Cre/+}$/*ROSA* embryos (Fig. 3 *G* and *I*) at e12.5, confirming that they indeed originate from Ascl1+/Ptf1a− progenitors.

It has been previously shown that in developing rh1, Phox2a specifically labels neurons of the locus coeruleus (LC) (30, 31), suggesting that the Phox2a+ cells we described at e12.5 were differentiating LC neurons. The identity of the Lmx1b+ cells in rh1 was less certain. To determine if they were extracerebellar neurons, we fate mapped them using *Lmx1b*^{LacZ} mice (32). Our analysis of e18.5 *Lmx1b*^{LacZ} embryos did not identify any β-gal staining within the cerebellar anlage (Fig. S4*A*), arguing that the Lmx1b+ lineage in rh1 does not give rise to cerebellar neurons. Previously, it has been shown in mouse embryos that Lmx1b and Tlx3 are coexpressed in a subset of neurons of the parabrachial (PB) nuclei (33), which develop independently of the RL (34). The rhombomeric origin of the PB nuclei is poorly understood. However, by analyzing e18.5 *En1*^{Cre}; *ROSA* embryos, in which most rh1-derived cells were labeled by β-gal expression (28), we found that virtually all Lmx1b+ PB neurons in these embryos were β-gal+ (Fig. S4 *B* and *C*), arguing that they originate from rh1. Together, these results raise a possibility that the Lmx1b+/Tlx3+ cells at e12.5 are differentiating neurons of the PB nuclei.

Thus, our expression and fate mapping studies in e12.5 mouse embryos strongly suggest that the Ascl1+/Ptf1a− domain located directly ventral to the Ptf1a+ cerebellar VZ gives rise to Phox2a+ and Lmx1b+ extracerebellar neuronal populations.

In *Ptf1a*$^{-/-}$ Embryos, Progenitors in the Cerebellar VZ Generate Extracerebellar Neurons That Normally Arise in More Ventral Neurepithelium. Next, we tested if in the absence of *Ptf1a* function the *Ptf1a*-expressing cerebellar VZ abnormally gives rise to Lmx1b+ and Phox2a+ cells. We found striking more than a twofold increase ($P = 0.0001$) in the number of Lmx1b+ cells in e12.5 *Ptf1a*$^{Cre/Cre}$ (*Ptf1a*$^{-/-}$) embryos compared with control littermates (Fig. S5). Furthermore, in *Ptf1a* mutants, the Lmx1b+ cells were clearly expanded dorsally, populating the length of the cerebellar anlage almost up to the RL (Fig. S5*B*, arrow). Interestingly, some of these ectopic Lmx1b+ cells were located adjacent to the mutant cerebellar VZ (Fig. S5 *A* and *B*, arrowheads), suggesting that in contrast to wild-type embryos, in *Ptf1a* mutants, Lmx1b+ cells were broadly generated in the cerebellar VZ.

To confirm that marker expression changes correlated with fate changes in *Ptf1a*$^{-/-}$ embryos, we conducted fate map analysis in *Ptf1a*$^{Cre/Cre}$;*Tau–nLacZ* mutants at e15.0. Because our earlier fate mapping in *Ptf1a* mutants revealed some differences in the

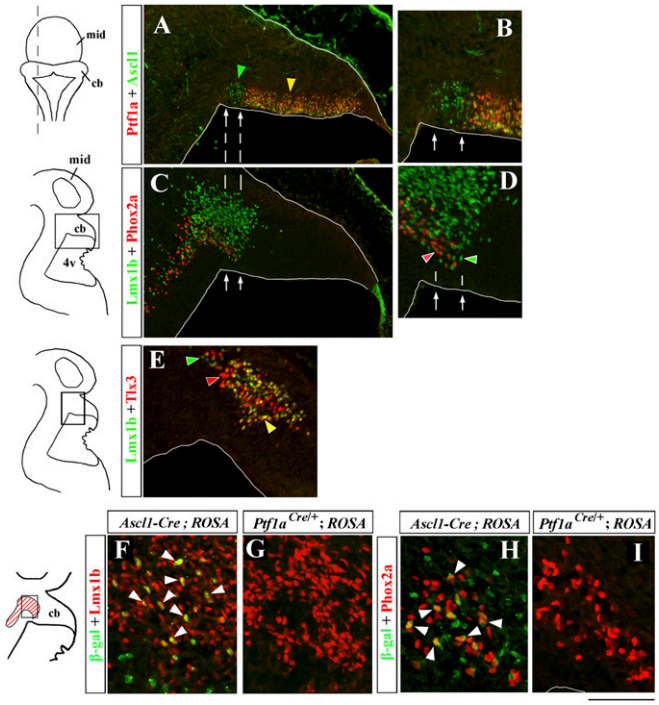

Fig. 3. The Ascl1+ domain located directly ventral to the *Ptf1a*-expressing cerebellar VZ gives rise to Phox2a+ and Lmx1b+ neurons. Sagittal sections of e12.5 cerebellar anlage regions, illustrated in schematics, stained with indicated antibodies. (*A–E*) Wild-type mouse embryos. (*A* and *C*) Adjacent sections showing dorsal and intermediate rh1. (*A*) The yellow arrowhead points to the Ptf1a+/Ascl1+ cerebellar VZ. The green arrowhead points to the Ascl1^{high}/Ptf1a− domain located directly ventral to the Ptf1a+/Ascl1+ cerebellar VZ. Right and left arrows point to the dorsal and ventral boundaries of the Ascl1^{high}/Ptf1a− domain, respectively (*A* and *C*). (*B* and *D*) Higher magnification of the area boxed in *A* and *C*, which corresponds to the Ascl1^{high}/Ptf1a− domain. Phox2a+ and Lmx1b+ neurons apparently streaming from the Ascl1^{high}/Ptf1a− domain are labeled by red and green arrowheads, respectively. (*E*) Many Lmx1b+ cells found in intermediate rh1 coexpressed Tlx3 (yellow arrowhead). The red arrowhead points to Tlx3+/Lmx1b− cells, and the green arrowhead points to Lmx1b+/Tlx3− cells, which were also present in this region. (*F–I*) Sagittal section from e12.5 *Ascl1-Cre/ROSA* (*F* and *H*) and *Ptf1a*$^{Cre/+}$*/ROSA* (*G* and *I*) embryos. In *Ascl1-Cre/ROSA* embryos, many Lmx1b+ cells and Phox2a+ cells were β-gal+ (yellow cells, arrowheads), suggesting that they originated from Ascl1+ progenitors. In *Ptf1a*$^{Cre/+}$*/ROSA* embryos, neither Lmx1b+ nor Phox2a+ cells expressed β-gal; thus, they did not originate from the Ptf1a+ cerebellar VZ. [Scale bar, 275 μm (*A* and *C*), 150 μm (*B*, *D*, and *E*), and 80 μm (*F–I*).]

distribution of β-gal+ cells in most medial rh1 compared with more lateral rh1, we first studied lateral serial sagittal sections. In *Ptf1a*$^{Cre/Cre}$*;Tau–nLacZ* (*Ptf1a*$^{-/-}$) embryos, the majority (82%) of β-gal+ cells, including those located both within and outside the mutant cerebellar anlage, expressed high levels of Lmx1b (Fig. 4 *D–G*). In contrast, in littermates with Ptf1a function (*Ptf1a*$^{Cre/+}$*;Tau–nLacZ*), β-gal+ cells did not express Lmx1b, and no Lmx1b+ cells were within the cerebellar anlage (Fig. 4 *A–C* and *G*). Furthermore, there was more than a twofold ($P = 0.001$) increase in the number of Lmx1b+ cells in *Ptf1a*$^{-/-}$ (*Ptf1a*$^{Cre/Cre}$*; Tau–nLacZ*) rh1 compared with control (*Ptf1a*$^{Cre/+}$*;Tau–nLacZ*) littermates (Fig. 4*H*). Notably, similar to e12.5, at e15.0, ectopic Lmx1b+ cells in the cerebellar anlage of *Ptf1a*$^{-/-}$ (*Ptf1a*$^{Cre/Cre}$*; Tau–nLacZ*) embryos were located along the entire length of the cerebellar VZ (open arrowhead in Fig. 4*E* and arrow in Fig. S6 *D* and *H*), excluding only its most dorsal part near the RL (open arrowhead in Fig. S6 *D* and *H*). These ectopic Lmx1b+ cells occupied a domain normally populated by Purkinje cells (Calbindin+ cells) and molecular layer interneuron progenitors (Pax2+ cells) in control embryos (Fig. S6 *A–F*, arrow). Interestingly, a small number of Calbindin+ Purkinje cells were still present in *Ptf1a* mutants, and some coexpressed Lmx1b (Fig. S6 *D*, *d–d''* and open arrowheads in *d–d''*), suggesting incomplete transformation. Thus, both our *Ptf1a* fate mapping and expression studies demonstrate that in the absence of Ptf1a function, the *Ptf1a*-expressing cerebellar VZ aberrantly gives rise to Lmx1b+ cells instead of Purkinje cells and molecular layer interneurons. Although some Lmx1b+ cells derived from the *Ptf1a*$^{-/-}$ cerebellar VZ were located within the cerebellum at e15.0, at lateral levels where cerebellum is continuous with pons, many occupied ectopic positions outside the cerebellar anlage.

Next, we analyzed the most medial region of rh1, where the cerebellar anlage is separated from more ventral neuroepithelium by the aqueduct (Fig. S7). Surprisingly, numerous ectopic Lmx1b+ cells were still detected in the medial cerebellar anlage (Fig. S7 *B* and *D*, arrow), and the vast majority of β-gal+ cells in the medial cerebellar anlage of e15.0 *Ptf1a*$^{Cre/Cre}$*;Tau–nLacZ* (*Ptf1a*$^{-/-}$) embryos were Lmx1b+ (Fig. S7*E*, arrowheads). Thus, although in *Ptf1a* mutants derivatives of the cerebellar VZ do not contribute to more ventral neuroepithelium in the most medial rh1, they still initiate expression of Lmx1b, an extracerebellar marker. Together these data show that Ptf1a is required to suppress Lmx1b expression throughout the entire M–L axis of the cerebellar anlage.

To determine if loss of *Ptf1a* leads to ectopic expression of an abnormal multigenic program that is not just limited to Lmx1b, we assessed the expression of Tlx3. Tlx3 is coexpressed with Lmx1b in neurons normally originating from the neuroepithelium just ventral of the *Ptf1a*-expressing cerebellar VZ. We observed more than a twofold ($P = 0.0003$) increase in the number of Tlx3+ cells in rh1 of e14.5 *Ptf1a*$^{-/-}$ embryos (*Ptf1a*$^{Cre/Cre}$ or *Ptf1a*$^{Cre/YFP}$) (Fig. 4 *I–O*). Further, ectopic Tlx3 staining was detected in the cerebellum in *Ptf1a*$^{-/-}$ but not control (*Ptf1a*$^{Cre/+}$ or *Ptf1a*$^{YFP/+}$) embryos (Fig. 4 *I* and *L*, open arrowhead). Colabeling experiments revealed that in *Ptf1a* mutants, the majority of Lmx1b+ cells coexpressed various levels of Tlx3 (Fig. 4*N*, arrowheads), including those located in ectopic positions in the cerebellum (Fig. 4*N*, open arrowhead). To further confirm that these ectopic Lmx1b+/Tlx3+ cells arose from the *Ptf1a* lineage, we analyzed *Ptf1a*$^{Cre/YFP}$ (*Ptf1a*$^{-/-}$) mutants, in which the *Ptf1a*-expressing cerebellar VZ was labeled by YFP expression from the *Ptf1a*^{YFP} allele. YFP/Lmx1b/Tlx3 colabeling revealed some triple-positive cells in the cerebellar VZ of *Ptf1a*$^{Cre/YFP}$ mutants (Fig. 4*N*, arrowheads), suggesting that in the absence of *Ptf1a* function, misspecification of cells begins even before they exit the cerebellar VZ.

Notably, loss of *Ptf1a* function did not alter production of Phox2a+ cells. In both *Ptf1a*$^{Cre/Cre}$*;Tau–nLacZ* (*Ptf1a*$^{-/-}$) mice and their *Ptf1a*$^{Cre/+}$*;Tau–nLacZ* littermates, Phox2a+ cells were β-gal− (Fig. S8). In addition, there was no increase in the number of Phox2a+ cells, and their location was unchanged in *Ptf1a* mutant embryos (Fig. S8). Together, these data indicate that loss of Ptf1a function causes the *Ptf1a*-expressing cerebellar VZ to specifically generate Lmx1b+/Tlx3+ cells rather than a broad spectrum of ventrally derived cells.

To study when the misspecified Lmx1b+ cells were generated in the *Ptf1a*$^{-/-}$ cerebellar VZ, *Ptf1a*$^{Cre/Cre}$*;Tau–nLacZ* (*Ptf1a*$^{-/-}$) mice were injected with BrdU at e12.0 and analyzed at e14.5. Some Lmx1b+ cells ectopically located in the cerebellar anlage were clearly BrdU+ (Fig. S9 *A–E*), and thus underwent their final mitosis around e12.0. Colabeling with β-gal confirmed that these Lmx1b+/BrdU+ cells indeed originated from the *Ptf1a* lineage (Fig. S9 *C–G*). These data argue that in *Ptf1a* mutants, at least some misspecified Lmx1b+ neurons ectopically arise in the *Ptf1a*-expressing cerebellar VZ as early during development as at e12.0.

Neurons Derived from *Ptf1a*-Expressing Progenitors Populate Brainstem and PB Nuclei in *Ptf1a*$^{-/-}$ Embryos. To determine the eventual fates of extracerebellar cells originating from the

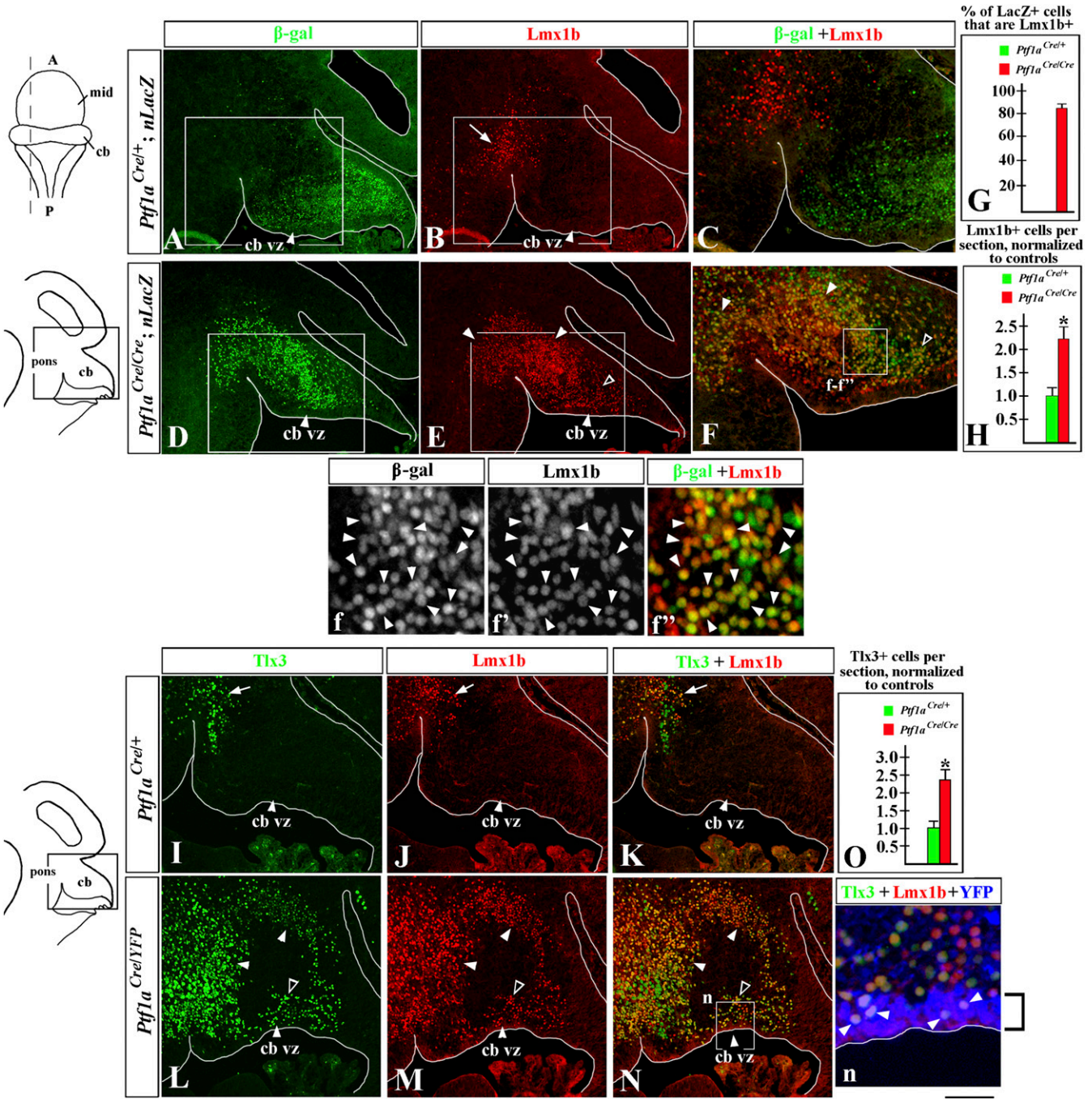

Fig. 4. *Ptf1a*-expressing cerebellar VZ produces Lmx1b+/Tlx3+ neurons in the absence of Ptf1a function. Sagittal sections of e15.0 (*A–F*) and e14.5 (*I–N*, *n*) rh1 regions, illustrated in schematics, stained with indicated antibodies. Magnified regions correspond to boxed areas of adjacent data panels. (*A–F*) In control (*Ptf1a*$^{Cre/+}$;*Tau–nLacZ*) embryos, Lmx1b+ cells were located ventral to the cerebellum (*B*, arrow) and were β-gal– (*C*). In *Ptf1a*$^{-/-}$ (*Ptf1a*$^{Cre/Cre}$;*Tau–nLacZ*) embryos, Lmx1b+ cells were increased in number (arrowheads in *E*) and many were found within the cerebellar anlage, adjacent to the cerebellar VZ (*E*, open arrowhead). The vast majority of β-gal+ cells in *Ptf1a* mutants were Lmx1b+ (arrowheads in *F* and *f–f''*), including those clearly located within the cerebellar anlage adjacent to the cerebellar VZ (*F*, open arrowhead). (*G*) Cell counts revealed that 82% of β-gal+ cells in *Ptf1a* mutants ($n = 4$ embryos), but none in control embryos ($n = 4$ embryos), expressed Lmx1b. (*H*) Cell counts revealed more than a twofold increase (*$P = 0.001$) in the number of Lmx1b+ cells in *Ptf1a* mutants compared with controls ($n = 4$ embryos per genotype). (*I–N*) In control (*Ptf1a*$^{Cre/+}$) embryos, Tlx3+ cells were located ventral to the cerebellum and many of them coexpressed Lmx1b (*I–K*, arrow). In *Ptf1a*$^{-/-}$ (*Ptf1a*$^{Cre/YFP}$) embryos, Tlx3+ cells were increased in number (arrowheads in *L*), and many were found within the cerebellar anlage adjacent to the cerebellar VZ (*L*, open arrowhead). The vast majority of Tlx3+ cells in *Ptf1a* mutants were Lmx1b+ (*N*, arrowheads), including those located within the cerebellar anlage adjacent to the VZ (*N*, open arrowhead). (*O*) Cell counts revealed more than a twofold increase (*$P = 0.0003$) in the number of Tlx3+ cells in *Ptf1a* mutants compared with controls ($n = 4$ embryos per genotype). (*n*) In *Ptf1a*$^{Cre/YFP}$ (*Ptf1a*$^{-/-}$) mutants, progenitors in the cerebellar VZ were labeled by YFP expression (bracket). Arrowheads point to Lmx1b/Tlx3/YFP triple-positive cells found in the *Ptf1a*-expressing cerebellar VZ in *Ptf1a*$^{Cre/YFP}$ (*Ptf1a*$^{-/-}$) mutants. [Scale bar, 200 μm (*A*, *B*, *D*, and *E*), 125 μm (*C* and *F*), 180 μm (*I–N*), and 40 μm (*f–f''* and *n*).]

Ptf1a-expressing cerebellar VZ in *Ptf1a* mutants, we studied *Ptf1a*$^{Cre/YFP}$;*Tau–nLacZ* (*Ptf1a*$^{-/-}$) mice at e18.5, the oldest viable age of *Ptf1a* null mice. Comparing sagittal sections taken at the same M–L levels from *Ptf1a*$^{Cre/YFP}$;*Tau–nLacZ* (*Ptf1a*$^{-/-}$) and

Ptf1a$^{Cre/+}$;*Tau–nLacZ* control embryos, we found fewer β-gal+ cells in the *Ptf1a*$^{-/-}$ cerebellum compared with control littermates (Fig. S10 *A* and *B*). Instead, the majority of β-gal+ cells in *Ptf1a*$^{Cre/YFP}$;*Tau–nLacZ* (*Ptf1a*$^{-/-}$) mice were found in the brainstem, in the area of PB nuclei (Fig. S10*B*, arrows). No significant β-gal staining was found in the PB area of control (*Ptf1a*$^{Cre/+}$;*Tau–nLacZ*) littermates (Fig. S10*A*). To determine if the mislocalized β-gal+ cells in *Ptf1a* mutants indeed adopted the PB neuronal fate, we performed marker analysis. In wild-type developing rh1, a subset of PB neurons express Lmx1b (33, 35), and a subset of these neurons coexpress Lmx1a (36). Furthermore, coexpression of Lmx1b and Lmx1a is specific to PB neurons, as their coexpression is not seen in any other rh1 population (36). In e18.5 *Ptf1a*$^{Cre/YFP}$;*Tau–nLacZ* (*Ptf1a*$^{-/-}$) mutant but not in *Ptf1a*$^{Cre/+}$;*Tau–nLacZ* control embryos, we found β-gal/Lmx1b double-positive cells within the PB nuclei area, and some of these cells also expressed Lmx1a (Fig. S10 *C* and *D*, *d–d''*). In contrast, in e18.5 *Ptf1a*$^{Cre/YFP}$;*Tau–nLacZ* (*Ptf1a*$^{-/-}$) embryos, β-gal+ cells did not express Phox2a, even those located adjacent to endogenous Phox2a+ LC neurons (Fig. S10 *E* and *F*). Thus, in the absence of Ptf1a function, *Ptf1a*-expressing progenitors in the cerebellar VZ adopt noncerebellar brainstem fates, including the fate of neurons of PB nuclei but not LC neurons.

Misspecified Cells Occupy Ectopic Positions in *Ptf1a*$^{-/-}$ Cerebellum. Because normally the *Ptf1a*-expressing cerebellar VZ produces Purkinje cells, and at e14.5 some Purkinje cells were still present in *Ptf1a* mutants (Fig. S6 *A–D*), we also studied Purkinje cells in *Ptf1a*$^{-/-}$ embryos at e18.5. Consistent with previously published data (23), some e18.5 *Ptf1a*$^{-/-}$ cerebella (2/7) completely lacked Purkinje cells, whereas just a few Calb+ Purkinje cells were found in others (5/7) (Fig. S6 *I* and *J*). By e18.5, in wild-type embryos, Purkinje cells were located in a band below the EGL (Fig. S6*I*, arrowheads). In e18.5 *Ptf1a* mutants, some Calb+ Purkinje cells occupied this position below the EGL (Fig. S6*J*, arrowhead). None of these cells coexpressed Lmx1b (Fig. S6 *l–l''*). However, many Calb+ Purkinje cells occupied ectopic positions close to the pons (Fig. S6*J*, open arrowhead). These cells aberrantly coexpressed Calb and Lmx1b (Fig. S6 *k–k''*), suggesting that activation

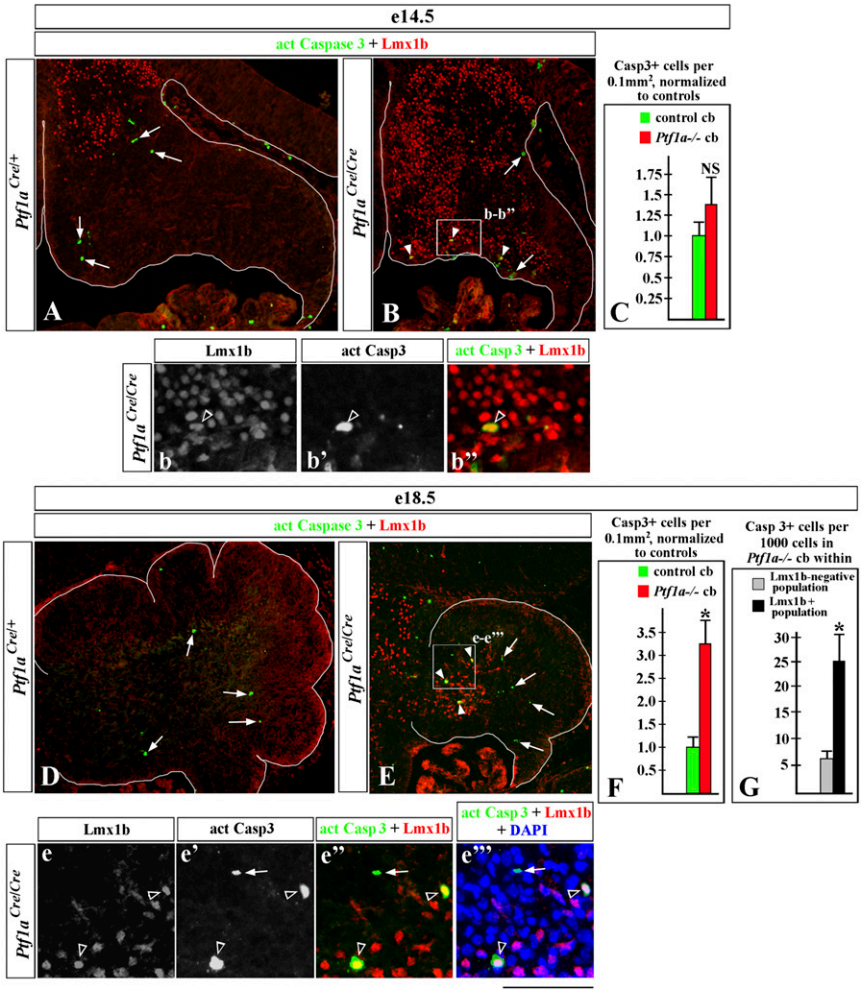

Fig. 5. Cell fate misspecification contributes to cell death in *Ptf1a*$^{-/-}$ cerebellum. Sagittal sections of e14.5 (*A*, *B*, and *b–b''*) and e18.5 (*D*, *E*, and *e–e'''*) cerebella with genotypes and antibody markers indicated. Magnified regions correspond to boxed areas in related data panels. Arrows point to Casp3+ cells found in both control (*A* and *D*) and *Ptf1a*$^{-/-}$ (*B*, *E*, and *e–e'''*) cerebella. Arrowheads point to Lmx1b+/Casp3+ cells found only in *Ptf1a*$^{-/-}$ cerebella (*B*, *b–b''*, *E*, and *e–e'''*). (*C* and *F*) Quantification of the numbers of Casp3+ cells per 0.1 mm^2 of cerebellar area in sagittal cerebellar sections from *Ptf1a* mutants ($n = 4$) and control embryos ($n = 4$) at e14.5 (*C*) and e18.5 (*F*). Apoptosis was significantly increased in *Ptf1a*$^{-/-}$ cerebella at e18.5 (*$P = 0.0017$) (*F*) but not at e14.5 (NS, nonsignificant; $P = 0.092$) (*C*). (*G*) Fractions of Casp3+ cells within the Lmx1b+ and Lmx1b− populations in e18.5 *Ptf1a*$^{-/-}$ cerebellum ($n = 4$ embryos). The fraction of Casp 3+ cells was ∼4 times higher (*$P = 0.005$) within the Lmx1b+ population in *Ptfa1a*$^{-/-}$ cerebellum compared with the Lmx1b− population in *Ptf1a*$^{-/-}$ cerebellum. Thus, misspecified Lmx1b+ cells die at a higher rate than Lmx1b− cells in e18.5 *Ptf1a*$^{-/-}$ cerebellum. [Scale bar, 200 μm (*A* and *B*), 60 μm (*b–b''* and *e–e'''*), and 275 μm (*D* and *E*).]

of the extracerebellar Lmx1b+ molecular program is incompatible with normal Purkinje cell migration.

Misspecification Precedes Apoptosis of Neurons Derived from the Cerebellar VZ in *Ptf1a*$^{-/-}$ Mice. Our data support the hypothesis that a fundamental cerebellar-to-extracerebellar fate switch is a primary cause of cerebellar agenesis in *Ptf1a* mutants. To evaluate other potential contributors to cerebellar agenesis, we studied proliferation and apoptosis. To assess proliferation, pregnant mice were injected with BrdU and their embryos were collected 1.5 h later. BrdU incorporation was not significantly different in the *Ptf1a*$^{-/-}$ cerebellar VZ compared with control littermates at either e12.5 or e14.5 (Fig. S11), indicating that reduced proliferation unlikely contributes to the cerebellar agenesis in *Ptf1a* mutants.

In contrast, increased apoptosis has been previously reported in *Ptf1a*$^{-/-}$ cerebellum (16, 23). Using activated Caspase 3 as a marker of apoptotic cells, we observed Lmx1b+/Casp3+ double-positive cells in *Ptf1a*$^{-/-}$ cerebella at both e14.5 and e18.5 (Fig. 5 *A*, *B*, *b–b''*, *D*, and *E*, *e–e''*), suggesting that some misspecified Lmx1b+ cells die. To better estimate when apoptosis becomes a significant contributor to the cerebellar agenesis phenotype, we evaluated the number of Casp3+ cells in sagittal cerebellar sections at two developmental stages. We found significantly more apoptotic cells in *Ptf1a*$^{-/-}$ relative to control cerebella at e18.5 ($P = 0.0017$), but no statistically significant differences at e14.5 ($P = 0.092$) (Fig. 5 *C* and *F*). Therefore, although some cells (including misspecified Lmx1b+ cells) die in *Ptf1a*$^{-/-}$ cerebella at e14.5, apoptosis is not a major contributor to cerebellar agenesis until later stages. Importantly, at e18.5, when apoptosis likely significantly contributes to *Ptf1a*$^{-/-}$ cerebellar agenesis, in *Ptf1a*$^{-/-}$ cerebella, the fraction of apoptotic cells within the Lmx1b+ cerebellar population was ~4 times higher ($P = 0.005$) compared with Lmx1b− cerebellar cells (Fig. 5 *e–e'''* and *G*). Thus, misspecified Lmx1b+ cells die in the *Ptf1a*$^{-/-}$ cerebellum at a higher rate compared with other cerebellar cells, suggesting that in some of these cells apoptosis is a secondary response to misspecification.

Discussion

Cerebellar agenesis is a rare, severe, and poorly understood human brain developmental phenotype. To date, homozygous loss-of-function mutations of *PTF1A*, encoding a bHLH transcription factor, are the sole known cause of this genetically heterogeneous disorder (20–22). Through analysis of *Ptf1a*$^{-/-}$ mouse models, we demonstrate that loss of *Ptf1a* causes a fundamental dorsal-to-ventral fate switch in rh1. Specifically, we show that in the absence of Ptf1a function, cells derived from the *Ptf1a*-expresing cerebellar VZ adopt the fate of more ventral extracerebellar cells as early as e12–e12.5. Our data support the conclusion that cerebellar agenesis in *Ptf1a* mutants results when misfated cells either exit the cerebellum to migrate into the brainstem or undergo subsequent apoptosis within the mutant cerebellar anlage at late embryonic stages.

***Ptf1a* Segregates Cerebellar Neurons from More Ventral Cell Fates.** Chick/quail transplant experiments located the cerebellar anlage in dorsal rh1 (37). The molecular mechanisms defining the cerebellar territory along the A–P axis of the developing neural tube have been well described (1, 2, 8, 19, 38). In contrast, until this report, the molecular mechanisms segregating the cerebellum from more ventral rh1 cell fates were unknown.

Ptf1a now represents the first gene known to regulate the ventral limit of the cerebellum. Genetic fate mapping studies were instrumental in demonstrating that the *Ptf1a*-expressing VZ in rh1 gives rise to cerebellar GABAergic cell fates, including Purkinje cells and molecular layer interneurons (16, 23). However, little was previously known regarding other more ventral progenitor domains in alar plate of rh1. We have now defined an Ascl1+/Ptf1a−, VZ domain located immediately ventral to the Ptf1a+ cerebellar VZ in rh1 alar plate. Its progeny initiate a Lmx1b+ genetic program and do not contribute to the cerebellum. Using *Ptf1a*^{Cre}/*ROSA* and *Ptf1a-Cre/Tau–nLacZ* alleles, we have demonstrated that the *Ptf1a*-expressing cerebellar VZ is distinct from this more ventral VZ domain and never generates Lmx1b+ lineages. In *Ptf1a* mutants, however, most *Ptf1a*-expressing cerebellar VZ progeny aberrantly activated the adjacent more ventral Lmx1b+ extracerebellar gene expression program as early as e12.5. By e14.5, many β-gal+ cells moved ventrally, exiting the cerebellar anlage to populate the brainstem (summarized in Fig. 6). A subset eventually became neurons of PB nuclei in *Ptf1a*$^{-/-}$ mice. The dorsal-to-ventral misspecification is widespread and spans the entire M–L axis of the *Ptf1a*$^{-/-}$ cerebellar anlage (Fig. 4 *A–F* and Fig. S7). In the most medial rh1, however, misspecified cerebellar cells did not shift ventrally beyond the cerebellar anlage (Fig. S7),

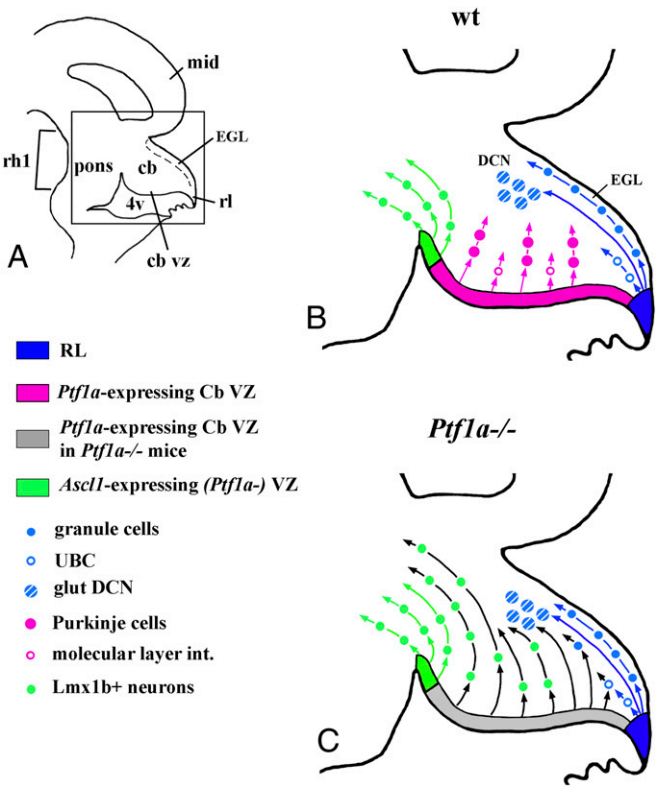

Fig. 6. Summary of cell fate misspecification in the *Ptf1a*$^{-/-}$ cerebellum. (*A*) Schematic of a sagittal section of an embryonic mid/hindbrain region. rh1, midbrain (mid), cerebellum (cb), pons, EGL, cerebellar VZ (cb vz), RL, and fourth ventricle (4v) are labeled. (*B* and *C*) Schematic of the region boxed in *A* in wild-type (WT) (*B*) and *Ptf1a*$^{-/-}$ (*C*) embryos. In wild-type embryos (*B*), the cerebellar RL (blue) gives rise to granule progenitors (small blue circles), glutamatergic neurons of the DCN (big hatched blue circles), and UBCs (open blue circles). The *Ptf1a*-expressing cerebellar VZ (magenta) gives rise to Purkinje cells (big magenta circles) and molecular layer interneurons (small open magenta circles). A Mash1+/Ptf1a− domain (green), located immediately ventral to the *Ptf1a*-expressing cerebellar VZ, gives rise to Lmx1b+ cells (green circles). Directions of cellular migrations and approximate migratory routes are indicated by arrows. All derivatives of the *Ptf1a*-expressing cerebellar VZ and the RL, mentioned above, remain in the cerebellum. Lmx1b+ neurons originating from the Mash1+/Ptf1a− domain exit the cerebellum and contribute to more ventral brainstem. (*C*) In the absence of the *Ptf1a* function, some cells derived from the *Ptf1a*-expressing cerebellar VZ (shown in gray) adopt the fate of granule cells (23) as well as glutamatergic neurons of the DCN and UBCs (this study). The vast majority of cells derived from the *Ptf1a*-expressing cerebellar VZ, however, initiate Lmx1b expression and many exit the cerebellar anlage contributing to more ventral brainstem.

possibly because at this level cerebellum is separated from pons by the aqueduct. The fate of these medial misspecified Lmx1b+ cells is not clear. Because in *Ptf1a* mutants the entire cerebellum degenerates (16, 23), one possibility is that these cells first migrate laterally and then exit the cerebellum at more lateral levels. Alternatively, they may remain in the cerebellum but die.

The wild-type neuroepithelium located directly ventral to the Ptf1a+ cerebellar VZ also gives rise to Phox2a+ LC neurons, in addition to Lmx1b+ neurons. In *Ptf1a*$^{-/-}$ animals, cells originating from the *Ptf1a*-expressing cerebellar VZ did not initiate expression of Phox2a and did not contribute to the LC. Therefore, in the absence of *Ptf1a*, the entire cerebellar anlage does not simply convert into more ventral neuroepithelium. Instead, loss of *Ptf1a* leads to a more nuanced misspecification of cells derived from the cerebellar VZ. Additional work is required to better define the mechanisms of this transformation.

Remarkably, in the spinal cord *Ptf1a* is required to segregate several classes of dorsal interneurons (dI): dI4 from more ventral dI5 interneurons at early stages of development and dIL(A) from dIL(B) neurons at later stages, in both cases repressing Lmx1b and Tlx3 expression (39–41). Developmentally, the cerebellum is very different from the spinal cord in terms of progenitor domains, morphogenetic movements, developmental timing, and both routes and modes of neuronal migration. Our study suggests, however, that the same *Ptf1a*-dependent program that is used in the developing spinal cord to segregate different classes of dorsal interneurons is also used to segregate cerebellar neurons from more ventral rh1 cell fates.

***Ptf1a* Also Segregates the Cerebellar VZ from the RL.** Although a majority of cells derived from the *Ptf1a*-expressing cerebellar VZ adopt more ventral extracerebellar fates in the absence of *Ptf1a* function, our data also support the previous observation that in *Ptf1a*$^{-/-}$ mice, some cerebellar VZ cells become granule cells (23). Furthermore, we extend these observations, demonstrating that loss of *Ptf1a* causes a limited number of cerebellar VZ cells to adopt additional RL fates—glutamatergic (Tbr1+) neurons of the DCN and UBCs (Fig. 6). Therefore, *Ptf1a* is also involved in segregation of the cerebellar VZ from a more dorsally located RL. Notably, in e14.5–e15.0 *Ptf1a* mutants, ectopic Lmx1b+ cells appeared along the entire length of the cerebellar VZ, excluding only its most dorsal part, adjacent to the RL (Fig. S6 *D* and *H*, open arrowhead). In contrast, many ectopic Pax6+ cells in *Ptf1a* mutants were found adjacent to this dorsal portion of the cerebellar VZ (Fig. 1*H*, open arrowhead). These data suggest that in *Ptf1a* mutants, most of the cerebellar VZ gives rise to Lmx1b+ extracerebellar cells, whereas its most dorsal segment produces RL derivatives.

Cerebellar Agenesis as a New, Dorsal-to-Ventral, Cell Fate Misspecification Phenotype in Humans. Similar to human patients, loss of *Ptf1a* in mice leads to cerebellar agenesis. Previous work suggested death of cerebellar cells as the major cause of cerebellar agenesis in *Ptf1a*$^{-/-}$ mice (16, 23). We concur that cell death is an important contributor to cerebellar agenesis in this mouse model. Notably, however, the *Ptf1a*$^{-/-}$ cerebellum is hypoplastic by e14.5, before the onset of extensive cell death at e16.5 (this study and ref. 23). The cell fate misspecification that we describe in the current study, however, already happens by e12–e12.5. By e14.5, in *Ptf1a* mutants, many cells originating from the *Ptf1a*-expressing cerebellar VZ were already located outside the cerebellum in the more ventral brainstem. Thus, extensive migration of misspecified cells away from the cerebellar anlage substantially reduces its size before increased cell death. In addition, although some Lmx1b+ misspecified cells remained in the cerebellum, many died at later stages, suggesting that death of some cells in *Ptf1a*$^{-/-}$ cerebellum is secondary to their earlier misspecification. Thus, our data argue that cell fate misspecification is a major cause of *Ptf1a*-related cerebellar agenesis.

To date, very few neuronal cell fate misspecification phenotypes have been described in humans. Perhaps the best known example is *SHH*-related holoprosencephaly, where loss of ventral forebrain tissue is likely caused by early ventral mispatterning of the anterior neural tube (42–45). Variable brainstem and neural crest-related phenotypes, likely caused by early A–P hindbrain rhombomere segmentation defects, have been reported in patients with homozygous *HOXA1* truncating mutations (46). The most recent recognized human example is CHARGE (coloboma of the eye, heart defects, atresia of the choanae, retarded growth and development, genital anomalies, and ear malformations or deafness) syndrome, where cerebellar vermis hypoplasia results from the A–P mispatterning of the midhindbrain region due to mutations in DNA binding protein gene *CHD7* and subsequent misexpression of several isthmus-related genes (47). In this study, we described a new type of dorsal-to-ventral cell fate misspecification, which is dramatic and widespread in the *Ptf1a*$^{-/-}$ mouse cerebellum. The fact that patients with cerebellar agenesis have homozygous mutations in the *PTF1A* gene suggests a severe cell fate misspecification during cerebellar development, likely comparable to that observed in *Ptf1a*$^{-/-}$ mice. Although complete cerebellar agenesis is rare in humans, the related but less severe phenotypes of cerebellar vermis hypoplasia and cerebellar hypoplasia are much more common. We hypothesize that partial cerebellar-to-brainstem transformations contribute to a subset of these milder human cerebellar malformations. We eagerly await the results of ongoing gene discovery experiments in human patient cohorts to validate this hypothesis.

Materials and Methods

The following mouse lines were used in this study: *Ptf1a*^{Cre} (in which the *Ptf1a* protein-coding region is replaced by that of *Cre* recombinase) (48), *Ptf1a*^{YFP} (in which the *Ptf1a* protein-coding region is replaced by that of *YFP*) (49), *En1*^{Cre} (28), *Ascl1-Cre* (*Ascl1-CIG*) (29), *Lmx1b*^{LacZ} (32), *ROSA26 LacZ* reporter (25), and *Tau–GFP–IRES–nLacZ* reporter (referred to as *Tau–nLacZ* nuclear reporter in this article) (27). All lines were maintained on a mixed genetic background and genotyped as previously described (25, 28, 29, 32, 48, 49). Because the *Ptf1a* protein-coding region is replaced by that of *Cre* recombinase or *YFP* in *Ptf1a*^{Cre} and *Ptf1a*^{YFP} alleles, respectively, we used *Ptf1a*$^{Cre/Cre}$ and *Ptf1a*$^{Cre/YFP}$ embryos to analyze cerebellar development and the fates of Ptf1a-expressing cells in the absence of *Ptf1a* function. All mouse procedures were approved by the Institutional Animal Care and Use Committees.

Immunohistochemistry, X-Gal staining, BrdU incorporation, and data analysis are described in *SI Materials and Methods*.

ACKNOWLEDGMENTS. We thank J. Johnson (University of Texas Southwestern Medical Center), C.V. Wright (Vanderbilt University Medical Center), M. Magnuson (Vanderbilt University School of Medicine), T. Glaser (University of Michigan), R.F. Hevner (Seattle Children's), J.F. Brunet (Institut de Biologie de l'Ecole Normale Supérieure), H. Edlund (University of Umea), M. German (University of California, San Francisco), T. Perlmann (Karolinska Institute), A. Joyner (Sloan–Kettering Institute), M. Goulding (Salk Institute), S. Arber (University of Basel), and R. Machold (New York University) for mice and reagents; C. Wang and J. Skibo for technical assistance; and M. Blank, P. Haldipur, and T. Zwingman for valuable comments on the manuscript. This work was supported by National Institutes of Health Grants R01 NS050386 and R01 NS072441 (to K.J.M.) and R21 NS077163 (to V.V.C.).

1. Wassarman KM, et al. (1997) Specification of the anterior hindbrain and establishment of a normal mid/hindbrain organizer is dependent on Gbx2 gene function. *Development* 124(15):2923–2934.
2. Broccoli V, Boncinelli E, Wurst W (1999) The caudal limit of Otx2 expression positions the isthmic organizer. *Nature* 401(6749):164–168.
3. Marshall H, et al. (1992) Retinoic acid alters hindbrain Hox code and induces transformation of rhombomeres 2/3 into a 4/5 identity. *Nature* 360(6406):737–741.
4. Chisaka O, Musci TS, Capecchi MR (1992) Developmental defects of the ear, cranial nerves and hindbrain resulting from targeted disruption of the mouse homeobox gene Hox-1.6. *Nature* 355(6360):516–520.

5. Mark M, et al. (1993) Two rhombomeres are altered in Hoxa-1 mutant mice. *Development* 119(2):319–338.
6. Barkovich AJ, Millen KJ, Dobyns WB (2007) A developmental classification of malformations of the brainstem. *Ann Neurol* 62(6):625–639.
7. Barkovich AJ, Millen KJ, Dobyns WB (2009) A developmental and genetic classification for midbrain-hindbrain malformations. *Brain* 132(Pt 12):3199–3230.
8. Sillitoe RV, Joyner AL (2007) Morphology, molecular codes, and circuitry produce the three-dimensional complexity of the cerebellum. *Annu Rev Cell Dev Biol* 23:549–577.
9. Wang VY, Rose MF, Zoghbi HY (2005) Math1 expression redefines the rhombic lip derivatives and reveals novel lineages within the brainstem and cerebellum. *Neuron* 48(1):31–43.
10. Machold R, Fishell G (2005) Math1 is expressed in temporally discrete pools of cerebellar rhombic-lip neural progenitors. *Neuron* 48(1):17–24.
11. Englund C, et al. (2006) Unipolar brush cells of the cerebellum are produced in the rhombic lip and migrate through developing white matter. *J Neurosci* 26(36): 9184–9195.
12. Fink AJ, et al. (2006) Development of the deep cerebellar nuclei: Transcription factors and cell migration from the rhombic lip. *J Neurosci* 26(11):3066–3076.
13. Wingate R (2005) Math-Map(ic)s. *Neuron* 48(1):1–4.
14. Hagan N, Zervas M (2012) Wnt1 expression temporally allocates upper rhombic lip progenitors and defines their terminal cell fate in the cerebellum. *Mol Cell Neurosci* 49(2):217–229.
15. Hunter NL, Dymecki SM (2007) Molecularly and temporally separable lineages form the hindbrain roof plate and contribute differentially to the choroid plexus. *Development* 134(19):3449–3460.
16. Hoshino M, et al. (2005) Ptf1a, a bHLH transcriptional gene, defines GABAergic neuronal fates in cerebellum. *Neuron* 47(2):201–213.
17. Hori K, Hoshino M (2012) GABAergic neuron specification in the spinal cord, the cerebellum, and the cochlear nucleus. *Neural Plast* 2012:921732.
18. Martinez S, Andreu A, Mecklenburg N, Echevarria D (2013) Cellular and molecular basis of cerebellar development. *Front Neuroanat* 7:18.
19. Basson MA, et al. (2008) Specific regions within the embryonic midbrain and cerebellum require different levels of FGF signaling during development. *Development* 135(5):889–898.
20. Sellick GS, et al. (2004) Mutations in PTF1A cause pancreatic and cerebellar agenesis. *Nat Genet* 36(12):1301–1305.
21. Tutak E, et al. (2009) A Turkish newborn infant with cerebellar agenesis/neonatal diabetes mellitus and PTF1A mutation. *Genet Couns* 20(2):147–152.
22. Al-Shammari M, Al-Husain M, Al-Kharfy T, Alkuraya FS (2011) A novel PTF1A mutation in a patient with severe pancreatic and cerebellar involvement. *Clin Genet* 80(2): 196–198.
23. Pascual M, et al. (2007) Cerebellar GABAergic progenitors adopt an external granule cell-like phenotype in the absence of Ptf1a transcription factor expression. *Proc Natl Acad Sci USA* 104(12):5193–5198.
24. Dymecki SM, Kim JC (2007) Molecular neuroanatomy's "Three Gs": A primer. *Neuron* 54(1):17–34.
25. Soriano P (1999) Generalized lacZ expression with the ROSA26 Cre reporter strain. *Nat Genet* 21(1):70–71.
26. Chizhikov VV, et al. (2010) Lmx1a regulates fates and location of cells originating from the cerebellar rhombic lip and telencephalic cortical hem. *Proc Natl Acad Sci USA* 107(23):10725–10730.
27. Hippenmeyer S, et al. (2005) A developmental switch in the response of DRG neurons to ETS transcription factor signaling. *PLoS Biol* 3(5):e159.
28. Corrales JD, Blaess S, Mahoney EM, Joyner AL (2006) The level of sonic hedgehog signaling regulates the complexity of cerebellar foliation. *Development* 133(9): 1811–1821.
29. Battiste J, et al. (2007) Ascl1 defines sequentially generated lineage-restricted neuronal and oligodendrocyte precursor cells in the spinal cord. *Development* 134(2): 285–293.
30. Parras CM, et al. (2002) Divergent functions of the proneural genes Mash1 and Ngn2 in the specification of neuronal subtype identity. *Genes Dev* 16(3):324–338.
31. Pattyn A, Goridis C, Brunet JF (2000) Specification of the central noradrenergic phenotype by the homeobox gene Phox2b. *Mol Cell Neurosci* 15(3):235–243.
32. Schweizer H, Johnson RL, Brand-Saberi B (2004) Characterization of migration behavior of myogenic precursor cells in the limb bud with respect to Lmx1b expression. *Anat Embryol (Berl)* 208(1):7–18.
33. Dai JX, Hu ZL, Shi M, Guo C, Ding YQ (2008) Postnatal ontogeny of the transcription factor Lmx1b in the mouse central nervous system. *J Comp Neurol* 509(4):341–355.
34. Gray PA (2008) Transcription factors and the genetic organization of brain stem respiratory neurons. *J Appl Physiol (1985)* 104(5):1513–1521.
35. Miller RL, et al. (2012) Fos-activation of FoxP2 and Lmx1b neurons in the parabrachial nucleus evoked by hypotension and hypertension in conscious rats. *Neuroscience* 218: 110–125.
36. Zou HL, et al. (2009) Expression of the LIM-homeodomain gene Lmx1a in the postnatal mouse central nervous system. *Brain Res Bull* 78(6):306–312.
37. Hallonet ME, Le Douarin NM (1993) Tracing neuroepithelial cells of the mesencephalic and metencephalic alar plates during cerebellar ontogeny in quail-chick chimaeras. *Eur J Neurosci* 5(9):1145–1155.
38. Zervas M, Blaess S, Joyner AL (2005) Classical embryological studies and modern genetic analysis of midbrain and cerebellum development. *Curr Top Dev Biol* 69: 101–138.
39. Glasgow SM, Henke RM, Macdonald RJ, Wright CV, Johnson JE (2005) Ptf1a determines GABAergic over glutamatergic neuronal cell fate in the spinal cord dorsal horn. *Development* 132(24):5461–5469.
40. Mizuguchi R, et al. (2006) Ascl1 and Gsh1/2 control inhibitory and excitatory cell fate in spinal sensory interneurons. *Nat Neurosci* 9(6):770–778.
41. Hori K, et al. (2008) A nonclassical bHLH Rbpj transcription factor complex is required for specification of GABAergic neurons independent of Notch signaling. *Genes Dev* 22(2):166–178.
42. Chiang C, et al. (1996) Cyclopia and defective axial patterning in mice lacking Sonic hedgehog gene function. *Nature* 383(6599):407–413.
43. Roessler E, et al. (1996) Mutations in the human Sonic Hedgehog gene cause holoprosencephaly. *Nat Genet* 14(3):357–360.
44. Belloni E, et al. (1996) Identification of Sonic hedgehog as a candidate gene responsible for holoprosencephaly. *Nat Genet* 14(3):353–356.
45. Fernandes M, Hébert JM (2008) The ups and downs of holoprosencephaly: Dorsal versus ventral patterning forces. *Clin Genet* 73(5):413–423.
46. Tischfield MA, et al. (2005) Homozygous HOXA1 mutations disrupt human brainstem, inner ear, cardiovascular and cognitive development. *Nat Genet* 37(10):1035–1037.
47. Yu T, et al. (2013) Deregulated FGF and homeotic gene expression underlies cerebellar vermis hypoplasia in CHARGE syndrome. *Elife* 2:e01305.
48. Kawaguchi Y, et al. (2002) The role of the transcriptional regulator Ptf1a in converting intestinal to pancreatic progenitors. *Nat Genet* 32(1):128–134.
49. Burlison JS, Long Q, Fujitani Y, Wright CV, Magnuson MA (2008) Pdx-1 and Ptf1a concurrently determine fate specification of pancreatic multipotent progenitor cells. *Dev Biol* 316(1):74–86.